



## Monitoring the thermal contribution of certain mortar additives as a way to optimize the energy performance of buildings

Jorge López-Rebollo<sup>a,\*</sup>, Natalia Nuño Villanueva<sup>a</sup>, Ignacio Martín Nieto<sup>a</sup>, Cristina Sáez Blázquez<sup>a</sup>, Susana Del Pozo<sup>a</sup>, Diego González-Aguilera<sup>a</sup>

<sup>a</sup> Department of Cartographic and Land Engineering, University of Salamanca, Higher Polytechnic School of Ávila, Hornos Caleros, 50, 05003 Ávila, Spain

### ARTICLE INFO

#### Keywords:

Mortar  
Additives  
Thermal properties  
Sustainable material  
Solar simulator

### ABSTRACT

Climate challenge requires developing approaches capable of improving the thermal capacities of building materials. These are the objectives of the new additive manufacturing industry in the building sector to mitigation of urban heat island. The objective of this work was to verify that the thermal properties of the additives are transferred to those of the final product, the mortar. For this purpose, several additives with different thermal conductivities, ranging from 0,038 to 130 W/m-K, were selected to include them in the matrix of a standard mortar with the same volume percentage. Once the mixtures were prepared, they were subjected to two thermal tests: a first thermal conductivity test, and a second heat transfer test. For the last test, a low-cost solar simulator was used to heat the mortar samples. Both the heating and cooling of the samples were monitored with a thermographic camera. After analysis, it was found that the mortar samples with additives modified their thermal behaviour by up to 30 % compared to the mortar sample without additives. These are encouraging results that open up new research possibilities that could materialize in studying the thermal behaviour of mortars with other kind of additives and with different dosage percentages.

### Introduction

The increasing concern about climate change and its devastating effects constitutes a stimulus pushing the research towards the identification of novel alternatives to decrease the world energy consumption. The possibilities of mitigating its undesired effects can no longer depend solely on the implementation of emission reduction policies; it is necessary to adopt coordinated measures on other fronts of action [1].

In the climate challenge, building sector must be considered as one of the main key players involved. According to the statistics of the International Energy Agency (IEA), the building sector is one of the largest energy consumers (40 % worldwide). Within this sector, 27 % of energy consumption belongs to residential buildings, with an associated CO<sub>2</sub> emission rate of 17 % of global emissions [2]. The large energy consumption by this sector results in a greater depletion of resources and greater pollution and degradation of the environment.

In this context, one of the undesirable effects produced by high energy consumption in buildings and by the thermal properties of their construction materials is the creation of Urban Heat Islands (UHI) that

significantly alter the environmental stability of these areas [3,4]. Therefore, the energy efficiency of buildings is today a primary objective of energy policies at regional, national, and international level [5]. Thus, different mitigation actions must be considered for the sustainable planning of urban spaces. In this sense, the inclusion of green areas has proven to be one of the fundamental favourable factors [6]. Lately, the inclusion of climate change mitigation measures in building construction procedures has also been considered. Ideally, a combination of measures to mitigate unwanted effects together with energy saving measures could even be proposed, such as the energy use approach based on the residual heat stored by the heat island effect [7,8].

Focusing on improving the energy efficiency of buildings, the development of novel construction materials is gaining increasing interest in industrial and domestic communities. In this sense, different solutions have been introduced to minimize heating and cooling loads through the building envelope towards more energy-efficient buildings [9]. In this context, the incorporation of Phase Change Materials (PCM) translates into significant energy savings [10,11]. Considering the specific requirements of each building, and with the aim of going a step

\* Corresponding author.

E-mail addresses: [jorge\\_lopez@usal.es](mailto:jorge_lopez@usal.es) (J. López-Rebollo), [id00816629@usal.es](mailto:id00816629@usal.es) (N.N. Villanueva), [nachomartin@usal.es](mailto:nachomartin@usal.es) (I.M. Nieto), [u107596@usal.es](mailto:u107596@usal.es) (C.S. Blázquez), [s.p.aguilera@usal.es](mailto:s.p.aguilera@usal.es) (S. Del Pozo), [daguilera@usal.es](mailto:daguilera@usal.es) (D. González-Aguilera).

<https://doi.org/10.1016/j.seta.2023.103268>

Received 24 February 2023; Received in revised form 26 April 2023; Accepted 29 April 2023

Available online 13 May 2023

2213-1388/© 2023 The Author(s). Published by Elsevier Ltd. This is an open access article under the CC BY-NC-ND license (<http://creativecommons.org/licenses/by-nc-nd/4.0/>).

further, the approach can be directed in two different ways. On the one hand, in some places, it will be preferable for the material to conduct and/or store heat more efficiently, while in other locations buildings can be configured to reduce the heat island effect. Different research works address the improvement of the thermal properties of mortars from the point of view of thermal conductive [12] or the absorption of solar radiation [13], including tests of materials for the thermal energy storage [14] without neglecting their mechanical properties [15]. Nevertheless, these studies mainly focus on extracting thermal properties without testing how the materials actually behave under real or simulated environmental conditions. Moreover, expensive and sometimes polluting materials are often added to achieve thermal improvements. This highlights the need to find a cost-effective and environmentally friendly solution that is monitored and tested in environmental conditions similar to those of its potential use.

To advance in this field, this research aims to evaluate the thermal behaviour of mortars with different additives that allow these construction materials to fulfil not only a structural function, but an energy function. With that objective, this work includes a series of commonly used thermographic analyses with promising results in other materials [16,17]. In this sense, a novel experiment is proposed that combines a low-cost solar simulator to reproduce the environmental conditions of use with the application of active thermography for monitoring its behaviour. The different composition of the mortar samples results in different thermal diffusivity and heat flux [18] which can be monitored by a thermographic camera. This technique is an improvement over point measurements in conventional studies as it allows full-field thermal measurements to be made to analyse the overall behaviour, obtaining results that are closer to reality.

Consequently, an experimental campaign is performed on mortars with different additives, subjecting them to conductivity and thermographic tests to analyse their thermal behaviour. After this Introduction, Section 2 describes these materials and techniques employed. In Section 3, the experimental results for each test performed are shown. A

discussion of the results is given in Section 4. Finally, in Section 5, the main conclusions are drawn about the suitability of using certain material as additives of mortar mixtures to modify their thermal behaviour, as well as discuss the feasibility of introducing these compounds in the construction industry.

**Materials and methods**

This work focuses on the use of additives particularly selected to alter the thermal properties of mortars. Once the additives materials for the mixtures were selected, samples for subsequent tests were prepared. Respecting the mortar setting period, the samples were first subjected to thermal conductivity test using the needle probe method [19]. Those samples that showed the desired thermal result in the first test were subsequently subjected to thermal distribution tests by means of a thermographic camera [20]. Fig. 1 shows a schematic diagram of the workflow followed.

*Selection of additives and sample preparation*

Due to the importance of the properties of construction materials in the energy aspect of buildings, trying to modify these in order to achieve a change in their thermal behaviour is an interesting and challenge aspect. In this line of research, mortar has been the construction material selected due to its wide use in the construction sector and because it is easy to mix with different additives.

For the selection of additives, some factors have been considered key. For example, the ease of obtaining them, the possibility of reusing them and giving them a second use, and even, in the case of additives of the same nature and different form (powder and liquid, for example), the possibility of using both types. In the latter case, it is interesting to analyse whether its form can cause different thermal behaviour in the mortar sample with such material. Finally, it should be mentioned that the additives used in this study cannot currently be used commercially.

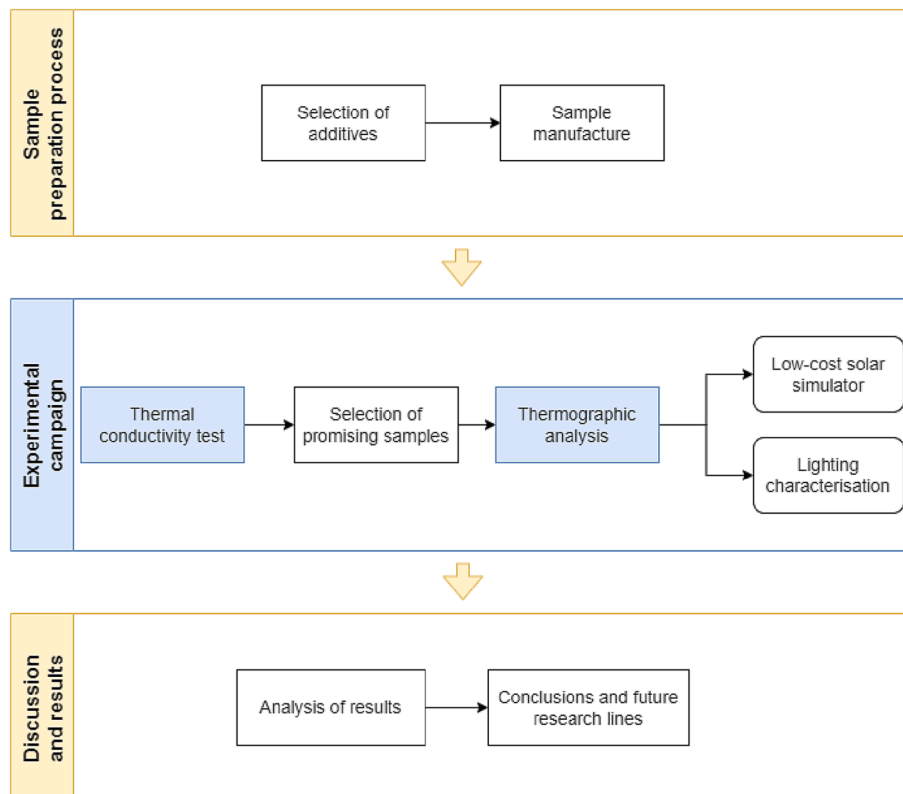


Fig. 1. Workflow diagram.

In this sense, five different materials were chosen to be added to the mortar as additives: polyester fibres, polystyrene, graphite, gypsum powder and crystallised gypsum. All of them are relatively easy to obtain and with the possibility of being reused in the construction industry.

Polyester fibres were chosen due to their high availability, and due to their possible reuse and have been used as an additive in photochromic mortars [21]. Polystyrene shares the key factors respect to the polyester fibres as it is commonly used in sample packaging and has been shown to influence cement for heat cycling [22]. Graphite is a mineral used in various industries such as the pharmaceutical industry, construction or even electrical industry (electrodes), so it would be another use given to this widely available material, already used in mortars with electromagnetic properties [23]. Gypsum, for its part, is a material commonly used in combination with cement [24] and that could be used as an additive in different forms. In this research its crystal and powder forms have been considered. Crystallised gypsum is its base mine form while the powdered form is the gypsum form that has been processed for its use in construction as moulding paste, as a bonding and joint paste, and even for artistic purposes. It is, therefore, a material that is present in the construction sector and that could be reused to improve the thermal properties of mortars.

Regarding the amount of additive to add to each mortar sample and given the variability in the nature and form of each one, it was decided to measure its amount in % volume so as not to exceed the amount of mortar used per sample. This would happen if the quantification method were mass, and in the specific case of additives such as polystyrene (low density). A value of 5% by volume of the total mixture was determined so that the mechanical properties of the resulting mortar are not altered. Taking into account the densities of the raw materials measured in the laboratory, the mortar mix compositions were 7 kg/m<sup>3</sup> for polyester fibre, 2,5 kg/m<sup>3</sup> for polystyrene, 105 kg/m<sup>3</sup> for graphite, 115 kg/m<sup>3</sup> for gypsum in its crystallised form and 60 kg/m<sup>3</sup> for powdered gypsum. Table 1 presents a summary with the characteristics of the additives used.

Once the additives have been selected and their quantity has been decided, the mortar base mix to which they will be added must be determined. In this study, the mortar was a mixture of natural siliceous aggregates, Portland cement and water in a ratio of 3:1:0,5 respectively. The characteristics of the components of the mortar mixture are the following:

- The cement used was white Portland cement with limestone (EN 197-1:2011 [28]) and a compressive strength of 42,5 N.
- The natural aggregates were siliceous sand treated with a 2 mm test sieve (UNE 7050-3 [29]).
- The sample water was non-aggressive according to UNE 83952 [30].

For the manufacture of the samples, prismatic moulds of 160 × 40 × 40 mm, described in the UNE-EN 196-1 standard [31], were used. The curing conditions were respected by keeping the samples in the moulds for the first 24 h. Subsequently the specimens were kept in water at a temperature of 293,15 ± 2 K.

A total of 18 samples were manufactured, so that three specimens were obtained for each of the six mixtures (5 with additives and 1

without additive). One of the three specimens per mixture was used for the thermal conductivity test, another for the heating-cooling tests, and the remaining one was kept for safety and for future research.

### Thermal conductivity procedure

The theoretical principle on which the thermal conductivity measurement procedure is based is known as the infinite line heat source theory, in which thermal conductivity is calculated from monitoring the dissipation of heat in the needle probe. Heat is injected to the needle for an established heating time  $t_h$ , and temperature is then measured in the monitoring needle during heating and for an extra time equal to  $t_h$  after heating. Equation (1) describes how the temperature during heating is obtained [32].

$$T = m_0 + m_2t + m_3 \ln t \tag{1}$$

Where  $m_0$  is the ambient temperature during the heating stage;  $m_2$  is the rate of background temperature drift; and  $m_3$  is the slope of a line relating temperature rise to logarithm of temperature.

The model during cooling is described in Equation (2).

$$T = m_1 + m_2t + m_3 \ln \frac{t}{t - t_h} \tag{2}$$

The thermal conductivity of the sample is finally obtained from Equation (3), which also considers the heat flux ( $q$ ).

$$k = \frac{q}{4m_3} \tag{3}$$

For carrying out the necessary measurements based on this principle on a laboratory scale, a DECAGON analyser was used: TEMPOS. This analyser complies with the following regulations that guarantee the standardization of the results: ISO 2008, ASTM 5334, IEEE 442 and is also capable of making accurate measurements not only of thermal conductivity but also of thermal resistance, specific heat, and thermal diffusivity of materials [33].






Considering the material of the samples and their size, the RK-3 needle was chosen due to its size sensor de 3,9 mm diameter y 60 mm length. This needle has a resistivity range of 17 to 1000 °C·cm/W and a conductivity range of 0.1 to 6 W/(m·K). Its accuracy is ± 10% from 0.1 to 6 W/(m·K).

For the thermal conductivity test with the described TEMPOS analyser, samples were radially drilled for the introduction of RK-3 needle. The contact between the needle and the material was ensured by inserting thermal grease in the mentioned hole.

Before the measuring process, RK-3 sensor was accordingly calibrated with the specific sample supplied by the manufacturer. Once calibrated, three measurements (of around 2 min each) were carried out on each mixture to evaluate possible measuring uncertainties and errors.

It should be also mentioned that ambient temperature was kept as constant as possible at 298,15 K during the measurement process to obtain the most accurate data possible. In this sense, to minimize these sources of error, about 15 min for samples and needle to equilibrate with the ambient temperature was required before taking measurements, and around 15 min between readings for temperatures to be equilibrated.

**Table 1**  
Summary table of additives, their thermal conductivity ( $\lambda$ ), and their image.

	Polyester	Polystyrene	Graphite	Gypsum (crystal)	Gypsum (powder)
$\lambda$ (W/m·K)	0,038 [25]	0,035 [26]	130 [27]	0,56 [26]	0,30 [26]
Image					



Heating test and temperature monitoring

The characterisation of thermal behaviour of the samples was carried out under active thermography and by a step heating approach. The procedure followed for these tests was as follows: i) design and manufacture of a low-cost solar simulator; ii) characterisation of the low-cost simulator; ii) set the configuration and calibration of the thermographic camera; and finally iv) perform the heating and cooling tests.

For that purpose, a low-cost solar simulator was used in order to replicate under laboratory conditions, the real state to which mortars can be subjected during their useful life. In this way, an attempt was made to manufacture a lighting system with similar characteristics to solar lighting using a metal arc halide lamp that simulates the heating produced by the sun's rays [34,35]. In this case, a Philips HPI-T Plus 250W/645 bulb was selected, so it was installed on a platform designed ad-hoc to hold it at different heights. A polished aluminium plate was used to concentrate the lighting on a lower surface to ensure uniformity and stability of the luminous flux.

In order to check the characteristics of the illumination obtained by the solar simulator, a Sekonic C7000 spectrometer was used to obtain its luminance, correlated colour temperature (CCT) and spectral power distribution (SPD). This device has a measurement range of 1 to 200.000 lx for illuminance with an accuracy of ± 5 %. The CCT allows values between 1.563 and 100.000 K to be obtained. Regarding the SPD, it is possible to obtain output wavelength increments of 1 nm in the range from 380 to 780 nm.

The monitoring of the temperature was carried out with a FLIR T540 thermographic camera. This camera integrates a 5 Mpx RGB sensor and a 464 × 348 px thermal sensor with a 42° lens along with a laser sensor that detects the distance between the object and the camera to improve focusing. The measuring temperature range is from 253,15 to 393,15 K with a temperature sensitivity < 30 mK at 303,15 K. In addition, it is possible to correct the emissivity in steps of 0,01 to adjust the temperature measurement according to the type of material.

The experimental campaign was carried out with the three samples selected after conductivity tests. In this way, the materials with the highest and lowest thermal conductivity were selected, in addition to the reference mortar. The tests for each material were carried out individually, placing the samples in such a way that the illumination had a vertical incidence on the surface to be studied, with a distance of 0,5 m. The camera was placed at the same distance with the least possible inclination to avoid errors in the measurement (Fig. 2a).

With the aim of guaranteeing the same initial conditions in each test, the samples were kept isolated at a temperature of 298,15 K until they were placed under the solar simulator. To ensure that the illumination was stable and to avoid deviations during heating, the lamp was turned on for 10 min until the sample was placed. Once the sample is placed, the thermographic image acquisition starts during the heating stage, with duration of 15 min. Once this time has elapsed, the solar simulator is switched off and the cooling stage begins, maintaining image acquisition for an additional 30 min. No additional device was used during this stage, so the sample was cooled by natural convection.

Regarding the acquisition of thermographic images, a frequency of 1 fps was used and taking into account heating and cooling, a total of 2700 images were acquired (45 min).

For each of these images, in order to evaluate if there were significant differences between the inside and outside of the sample due to edge effects, three Region of Interest (ROI) were selected (Fig. 2b): i) full sample, corresponding to the entire study surface; ii) edges, corresponding to the outer region with a width of 10 mm; and iii) centre, corresponding to the inner area with dimensions of 60 × 20 mm.

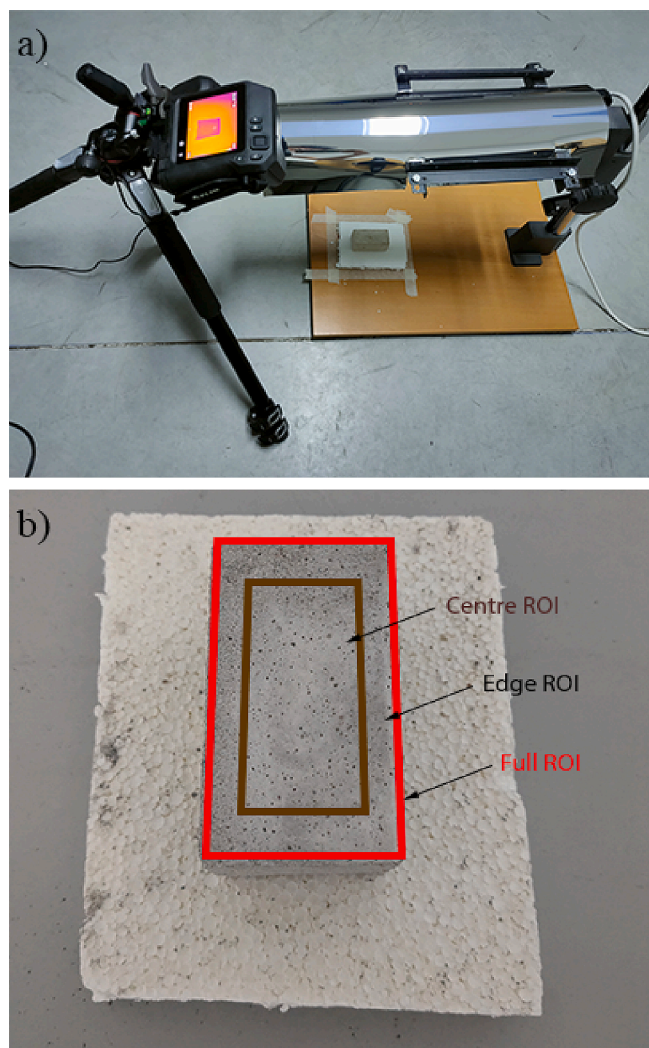


Fig. 2. Heating and cooling test. a) Test set up; b) Selected ROIs for thermographic analysis.

Experimental results

Thermal conductivity

The thermal conductivity test was carried out for all the samples, including the reference mortar and the five mortars with additives. For each of the samples, three tests were performed in order to eliminate possible uncertainties or measurement errors, so that a total of 18 tests were performed. Thermal conductivity and thermal resistance were obtained in each of these measurements and their results are shown in Table 2.

The results show differences between thermal conductivity and thermal resistance for mortars with different additives with respect to

Table 2 Results of the thermal conductivity and thermal resistance of the samples.

Sample	Thermal conductivity (W/m-K)		Thermal resistance (m-K/W)	
	$\bar{x}$	$\delta$	$\bar{x}$	$\delta$
Mortar	0,584	0,041	1,717	0,121
Polyester	0,386	0,027	2,603	0,178
Polystyrene	0,912	0,025	1,097	0,032
Graphite	0,861	0,087	1,170	0,114
Gypsum (C)	1,061	0,177	0,959	0,155
Gypsum (P)	0,446	0,042	2,257	0,210

the reference mortar. Taking into account that the difference for some materials is not very high, it was decided to select the two samples with the most extreme behaviours: mortar with crystallised gypsum as the mixture with the highest thermal conductivity and mortar with polyester fibres as the mixture with the lowest thermal conductivity. Along with them, the mortar without additives was kept as reference material to carry out the heating and cooling tests.

### Heating test and temperature monitoring

In order to carry out the heating and cooling test properly, the first step was to characterise the low-cost solar simulator. The lamp was switched on and its behaviour during the first 15 min was analysed with the spectrometer. The results for CCT are shown in Fig. 3a, while the corresponding results for luminance can be seen in Fig. 3b.

After 6 or 7 min a stable CCT of approximately 5600 K and a constant luminance of 22000 lx is reached. Nevertheless, it was decided to set a more conservative lamp warm-up time of 10 min to avoid possible disturbances. Thus, it is considered that once this time is reached the illumination is sufficiently stable that the samples can start to heat up homogeneously both spatially and temporally.

Once this stable illumination was achieved, the SPD normalised to 1 shown in Fig. 4 was obtained. A peak wavelength of 537 nm was obtained, together with two other peaks at wavelengths 453 nm and 549 nm with a value close to it.

The tests were analysed using two different approaches. On the one hand, the temperature evolution curve was analysed, both in the heating and cooling phases in order to study the differences in the behaviour of each material. On the other hand, the ROIs described above were studied to determine the possible influence of edge effects and effectiveness of

the heating device.

The heating and cooling curves (Fig. 5) were obtained for each of the samples. For this purpose, the mean value of the full ROI was calculated for each of the thermal images to eliminate point errors or defective pixels. Then, a moving average filter was applied to eliminate anomalous values caused by erroneous frames or measurement disturbances.

Once the curves were plotted, the values corresponding to the end of heating and cooling were extracted. These values correspond to the maximum temperature increase and the final temperature variation of the sample (Table 3). In order to study the possible temperature differences between the inside and outside of the samples, the analyses described in Section 2.3. and exemplified in Fig. 2b were performed.

## Discussion

### Thermal conductivity

The study of thermal conductivity and thermal resistance showed the differences produced by the introduction of additives in the manufacture of the mortars. Compared to the reference mortar, with a value of 0,584 W/m·K for thermal conductivity and 1,717 m·K/W for thermal resistance, the influence of the materials is detailed below:

- The mortar additivated with polyester fibres obtained the lowest thermal conductivity, with a decrease of 0,199 W/m·K. In addition, the thermal resistance was also 0,89 m·K/W higher with respect to the reference mortar. In this case, the low thermal conductivity of the additive was also transferred to the result of the mortar.
- Initially, polystyrene had a similar thermal conductivity to polyester fibres. Nevertheless, an opposite effect occurred, so that the thermal

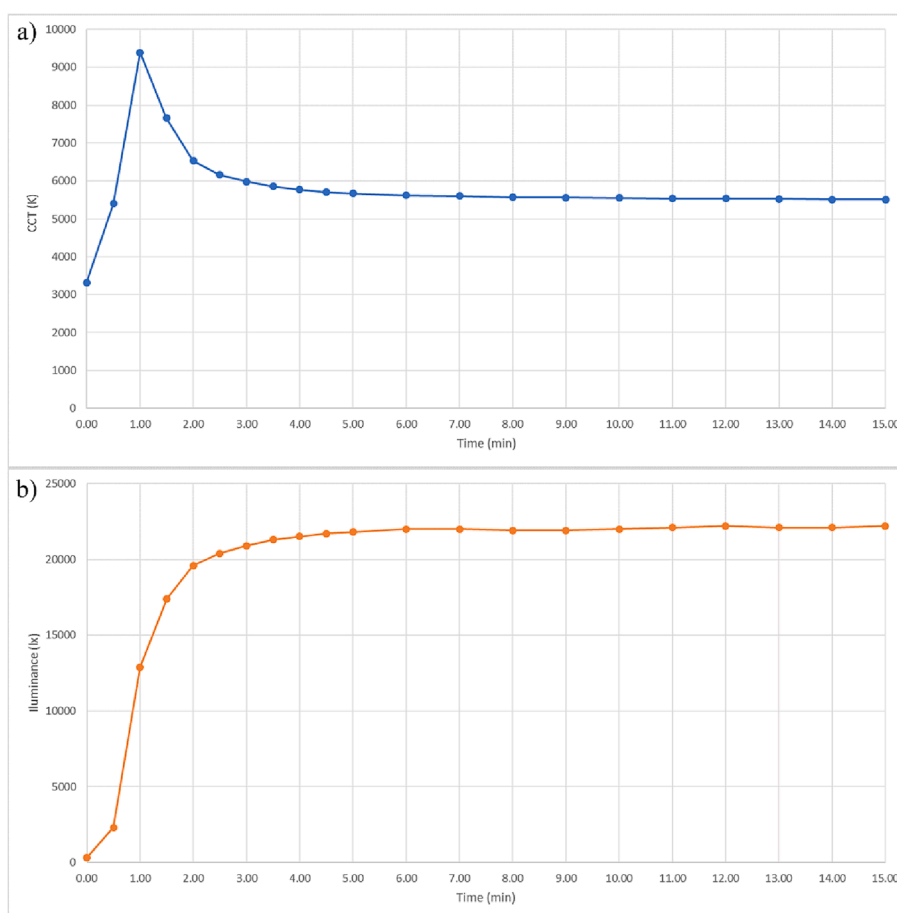


Fig. 3. Behaviour of the solar Simulator during the first 15 min. a) Correlated colour temperature (CCT); b) Luminance on the sample platform.

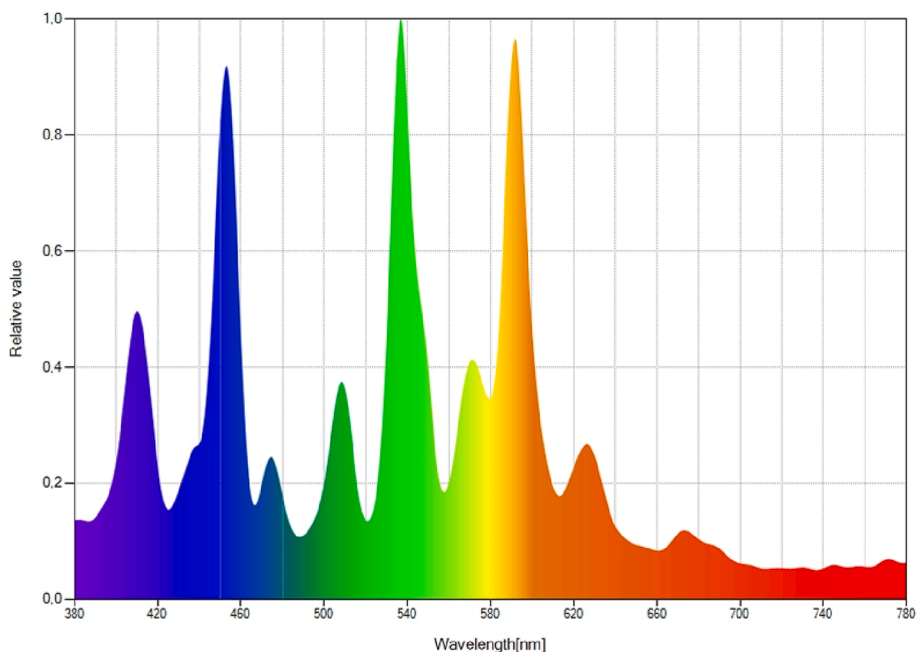


Fig. 4. Spectral power distribution of the solar simulator with stable illumination.

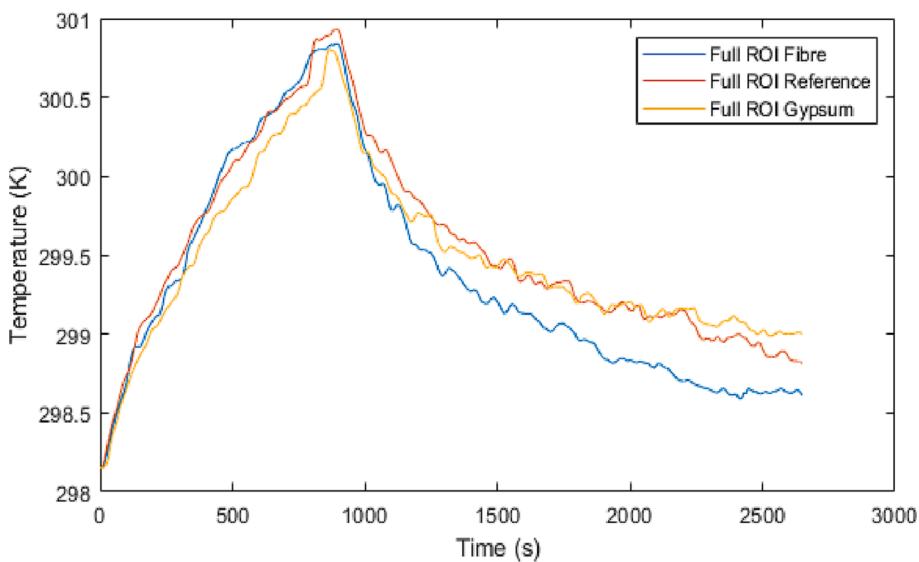


Fig. 5. Heating and cooling curves of thermal tests.

Table 3

Results for the heating and cooling tests for each ROI.  $\Delta T_M$  refers to maximum temperature increase.  $\Delta T_F$  refers to final temperature variation. \*Temperature increase in K.

Sample	Full ROI		Centre ROI		Edge ROI	
	$\Delta T_M$	$\Delta T_F$	$\Delta T_M$	$\Delta T_F$	$\Delta T_M$	$\Delta T_F$
Fibre	2,69	0,46	2,70	0,50	2,68	0,41
Reference	2,78	0,66	2,79	0,72	2,76	0,61
Gypsum	2,65	0,85	2,65	0,89	2,64	0,80

conductivity of the mortar with this additive increased with respect to the reference mortar in 0,328 W/m-K. Furthermore, the thermal resistance was reduced in 0,62 m-K/W. In this case, the shape and arrangement of the particles as well as their interaction with the mortar may be the cause of this effect.

- Graphite was initially the material with the highest conductivity of the selected materials by a considerable margin. Nevertheless, although its mixture was able to increase the thermal conductivity in 0,276 W/m-K and to reduce the thermal resistance in 0,547 m-K/W, it was not the most influential additive and did not reach the most extreme values.
- Beforehand, gypsum in its crystalline form had a thermal conductivity similar to that of the mortar. Nevertheless, the mixture of both reached the highest value for thermal conductivity with an increase of 0,476 W/m-K and the lowest thermal resistance with a decrease of 0,76 m-K/W, both referred to the reference mortar.
- Powdered gypsum had a slightly lower thermal conductivity than the mortar and was the material that produced the least changes in the mortar, reducing its thermal conductivity in only 0,139 W/m-K and increasing its thermal resistance in 0,54 m-K/W. Although its initial value was practically similar to that of crystalline gypsum, it has

been shown that the different forms in which the same material is presented can produce notable differences.

This study allowed obtaining a valid approximation for the thermal conductivity in order to select the samples with the most extreme behaviour as mentioned above. In the case of polyester fibres, which for the dosage studied ( $7 \text{ kg/m}^3$ ) manage to reduce the thermal conductivity of the mortar by 34 %, it has been estimated that the cost of one  $\text{m}^3$  of mortar is increased by 15 %. It is worth mentioning that, for the elderly, betting on the use of polyester fibres from, for example, the reuse of industrial bags made with this material is presented as a highly economical, sustainable and environmentally friendly option in the circular economy framework. This measure offers not only a solution that minimizes the problems associated with recycling these materials, but also allows for a more complete and responsible approach in terms of resource management and reduction of environmental impact.

For its part, crystallized gypsum, which for the dosage studied ( $115 \text{ kg/m}^3$ ) manages to increase thermal conductivity by 82 %, has a high cost associated with great variability depending on its origin, method of extraction and purity. In this sense, due to the high quantity required, its use as a mortar additive would be limited to specific cases in which the energy benefits derived from its application are associated with economic benefits higher than the manufacturing cost.

#### *Thermal behaviour*

The characterisation of the solar simulator made it possible to analyse its temporal behaviour in order to determine the time required to achieve stable illumination. In the case of the CCT, during the first minute, a maximum value of 9388 K is reached and then it begins to drop to a temperature of approximately 5600 K, which remains stable after approximately 7 min. The luminance also undergoes the greatest increase during the first two minutes, and after approximately 6 min it remains constant with a value of 22000 lx. As mentioned above, in order to avoid possible changes in the conditions that could modify this behaviour and delay the stabilisation time, it was decided to adopt a more conservative time of 10 min to start the heating tests. The SPD study showed a similar behaviour to that defined by the manufacturer and which is close to the real behaviour of sunlight.

With regard to heating test and temperature monitoring, the curves for each of the materials are practically similar in the heating phase, reaching a similar maximum temperature increase. The slight differences in this value are barely significant (0,1 K) and may be due to causes associated with the measurement process, such as the slight thermal oscillations caused by natural convection. In this sense, it must be considered that the heating is produced by radiation and that only surface heating is produced because the time is not very long, so it is difficult for the difference in conductivity to have an influence.

In the case of the cooling phase, significant differences can be observed. There is a difference of 0,4 K between the fibre sample and the crystallised gypsum sample, corresponding to those with the lowest and highest conductivity respectively. The reference sample is practically equidistant between the two. Due to the fact that the heating is carried out by radiation and in a short period of time as mentioned above, there is mainly surface heating, which means that the difference in conductivity does influence the final temperature of the sample in this case. In the case of the mortar with fibre, as it has a lower conductivity, the heating is only superficial without heating the whole sample, which causes a greater reduction in temperature during the cooling phase. On the other hand, the sample corresponding to the mortar with crystallised gypsum can heat up inside due to the higher conductivity, not only being a superficial heating. In this case, the heating of the whole sample causes the final surface temperature to be higher.

Regarding the edge effect test, the results show a similar behaviour during the heating phase as the difference between the centre and edge region does not exceed 0,03 K in any case. Edge effects were not visible

during the heating phase and it seems reasonable to assume that the heating of the solar simulator is homogeneous, since the temperature of the sample does not show spatial irregularities.

In the case of the results for the final temperature, differences can be seen between the temperatures corresponding to the central region and the edge region, while the temperatures for the full ROI are logically situated between the two. In this case, the differences reach 0,1 K, so that the edge ROI cools more than the centre ROI in all cases.

#### **Conclusions**

This research has sought to influence basic construction materials, such as mortar, in terms of their thermal properties through the use of additives for their future adaptation to the needs of use. This is an advantage not only in terms of energy efficiency, but considering the type of additives selected; it results in cost savings in materials and promotes sustainability within the construction ecosystem.

The additives that have generated the greatest variations in the thermal properties of the final mortar mix were: polyester fibres, achieving a 34 % reduction in thermal conductivity; and gypsum in its crystallised form, which achieved a thermal conductivity value 82 % higher, being the highest among the mixtures manufactured, although the value of the additive is similar to that of the mortar.

The first analysis on the two selected additives has been a heating-cooling test carried out with a low-cost solar simulator that has been characterized using a spectrometer, which determined an optimal heating time of 10 min. After this time, the illumination is considered stable with a CCT of 5600 K and a luminance of 22,000 lx with a peak wavelength of 453 nm.

The heating and cooling test allows the extreme thermal behaviour of the mortar to be analysed. Differences were found in the cooling phase of the test where the mixture with fibres acted as an insulator and caused the surface temperature variation at the end of the test to be 30 % lower than the reference sample, while for the mixture with crystallised gypsum this variation was 29 % higher than the reference sample. Regarding the heating phase, there were no significant differences.

The next test carried out was the analysis of the possible influence of the edge effect. The results showed that the heating device produced homogeneous heating and hardly affected the spatial distribution of temperatures. Nevertheless, there was more cooling at the edges of the sample, which will require increasing the sample size and differentiating between the two areas in future tests.

Therefore, the influence of the selection and use of additives on the thermal behaviour of the mortar is highlighted. In many cases, the desired effect will be thermal insulation of the exterior, in order to promote sustainability in the building ecosystem and to contribute to savings in building heating/cooling systems. The application of the materials with the lowest conductivity studied as cladding for buildings could result in a decrease in their temperature during cooling periods (night) and the consequent decrease in the heating-cooling sequence by starting from a lower initial temperature, thus contributing to the reduction of the heat island effect in cities. On the other hand, there are applications of ceramic and stone materials where the ability to transmit heat or to reduce the temperature as quickly as possible is important. An example of this is the backfilling of geothermal heat boreholes, where the aim is to allow the heat to pass from the ground to the borehole heat exchangers as quickly as possible. Another example can be found in service structures in cities with high summer temperatures, it is desirable that as the sun goes down their temperature is reduced more quickly to mitigate the heat island effect, increase their functional life and allow their use (e.g. street furniture benches, pavements, railings, etc.).

In both cases, it can be considered that the work yields promising results for the sector that motivate the continuation of this line of research. Future work will focus on carrying out more exhaustive analyses of the behaviour of these materials, carrying out tests with different



configurations. In this sense, it will be interesting to check their behaviour over longer heating–cooling times, and it will also be possible to carry out thermal profile studies to analyse temperatures at different depths.

### CRedit authorship contribution statement

**Jorge López-Rebollo:** Methodology, Investigation, Formal analysis, Writing – original draft, Writing – review & editing. **Natalia Nuño Villanueva:** Conceptualization, Investigation, Formal analysis, Writing – review & editing. **Ignacio Martín Nieto:** Investigation, Formal analysis, Writing – review & editing. **Cristina Sáez Blázquez:** Investigation, Formal analysis, Writing – review & editing. **Susana Del Pozo:** Investigation, Formal analysis, Writing – review & editing. **Diego González-Aguilera:** Supervision, Funding acquisition, Writing – review & editing.

### Declaration of Competing Interest

The authors declare that they have no known competing financial interests or personal relationships that could have appeared to influence the work reported in this paper.

### Data availability

Data will be made available on request.

### Acknowledgements

The authors want to thank the Spanish Ministry of Education, Culture and Sports for providing an FPU grant (Training Program for Academic Staff) to the corresponding author of this paper (grant number FPU20/01376). This work was financed by ERDF funds and Junta de Castilla y León through the TCUE 2021–2023 program within the framework of the DACHARAP project (N° Ref. PC-TCUE21-23\_033).

### References

- Medved S, Medved S. Urban environment and local climate. Building physics: heat, ventilation, moisture, light, sound, fire, and urban microclimate. 2022;453-72 3030743896.
- Afolabi LO, Ariff ZM, Megat-Yusoff PSM, Al-Kayiem HH, Arogundade AI, Afolabi-Owolabi OT. Red-mud geopolymer composite encapsulated phase change material for thermal comfort in built-sector. Sol Energy 2019;181:464–74. 0038-092X.
- Halder B, Bandyopadhyay J, Banik P. Evaluation of the climate change impact on urban heat island based on land surface temperature and geospatial indicators. Int J Environ Res 2021;15:819–35. 1735-6865.
- Kim SW, Brown RD. Urban heat island (UHI) intensity and magnitude estimations: A systematic literature review. Sci Total Environ 2021;779:146389. 0048-9697.
- Mirabella N, Roeck M, Ruschi Mendes Saade M, Spirinckx C, Bosmans M, Allacker K, et al. Strategies to improve the energy performance of buildings: A review of their life cycle impact. Buildings 2018;8:105. 2075-5309.
- Shishegar N. The impact of green areas on mitigating urban heat island effect: A review. Int J Environ Sustain. 2014;9:119-30 2325-1077.
- Jiang Y, Huang J, Shi T, Wang H. Interaction of urban rivers and green space morphology to mitigate the urban heat island effect: Case-based comparative analysis. Int J Environ Res Public Health 2021;18:11404. 1660-4601.
- Gao M, Chen F, Shen H, Barlage M, Li H, Tan Z, et al. Efficacy of possible strategies to mitigate the urban heat island based on urbanized high-resolution land data assimilation system (U-HRLDAS). J Meteorol Soc Japan Ser II 2019;97(6):1075–97. 0026-1165.
- Lotfabad P, Hançer P. A comparative study of traditional and contemporary building envelope construction techniques in terms of thermal comfort and energy efficiency in hot and humid climates. Sustainability. 2019;11:3582, 2071-1050.
- Alam M, Zou PXW, Sanjayan J, Ramakrishnan S. Energy saving performance assessment and lessons learned from the operation of an active phase change materials system in a multi-storey building in Melbourne. Appl Energy 2019;238: 1582–95. 0306 2619.
- Nada SA, Alshaer WG, Saleh RM. Thermal characteristics and energy saving of charging/discharging processes of PCM in air free cooling with minimal temperature differences. Alexandria Eng J. 2019;58:1175-90 10-0168.
- Corinaldesi V, Mazzoli A, Moriconi G. Mechanical behaviour and thermal conductivity of mortars containing waste rubber particles. Mater Des 2011;32: 1646–50. 0261-3069.
- López-Rebollo J, Del Pozo S, Nieto IM, Blázquez CS, González-Aguilera D. Experimental study on the thermal properties of pigmented mortars for use in energy efficiency applications. J Clean Prod 2023;382:135280. 0959-6526.
- Rathore PKS, Shukla SK, Gupta NK. Synthesis and characterization of the paraffin/expanded perlite loaded with graphene nanoparticles as a thermal energy storage material in buildings. J Sol Energy Eng 2020;142:041006. 0199-6231.
- Berardi U, Gallardo AA. Properties of concretes enhanced with phase change materials for building applications. Energy Buildings 2019;199. 402-14 0378 7788.
- Lizaranzu M, Lario A, Chiminelli A, Amenabar I. Non-destructive testing of composite materials by means of active thermography-based tools. Infrared Phys Technol 2015;71:113–20. 1350-4495.
- Rodríguez-Martín M, Fueyo JG, Pisonero J, López-Rebollo J, González-Aguilera D, García-Martín R, et al. Step heating thermography supported by machine learning and simulation for internal defect size measurement in additive manufacturing. Measurement 2022;205:112140. 0263-2241.
- Maldague X. Theory and practice of infrared technology for nondestructive testing. 2001.
- Yun TS, Jeong YJ, Han T-S, Youm K-S. Evaluation of thermal conductivity for thermally insulated concretes. Energy Build 2013;61:125–32. 0378-7788.
- Holland SD, Reusser RS. Material evaluation by infrared thermography. Annu Rev Mat Res 2016;46:287–303. 1531-7331.
- Sikandar MA, Mubeen G, Baloch Z, El-barbary AA, Hamad M. Comparative study on the performance of photochromic cement, epoxy, and polyester mortars. J Build Eng 2023;70:106394. 2352-7102.
- Ferrández-Mas V, García-Alcocel E. Durability of expanded polystyrene mortars. Constr Build Mater. 2013;46:175-82 0950-618.
- Stefaniuk D, Sobótka M, Jarczewska K, Logoń D, Majcher K, Musiał M, et al. Microstructure properties of cementitious mortars with selected additives for electromagnetic waves absorbing applications. Cem Concr Compos 2022;134: 104732. 0958-9465.
- Silva DBP, Lima NB, Lima VME, Estolano AML, Nascimento HCB, Vilemen P, et al. Producing a gypsum-based self-leveling mortar for subfloor modified by polycarboxylate admixture (PCE). Constr Build Mater 2023;364:130007. 0950-0618.
- Ceimat. Fibras poliester no tejidas. Available online: <https://ceimates/es/productos/producto-2> [Accessed February 20, 2023].
- Fomento Md. Catálogo de Elementos Constructivos del CTE (CEC). España 2011.
- GmbH GN. Propiedades grafito. Available online: <https://www.gab-neumann.com/Grafito-impermeable-Propiedades> [Accessed February 20, 2023].
- AENOR. UNE-EN 197-1. Cement - Part 1: Composition, specifications and conformity criteria for common cements. Madrid, Spain2011.
- AENOR. UNE 7050-3. Test sieves. Technical requirements and testing. Part 1. Test sieves of metal wire cloth. Madrid, Spain1997.
- AENOR. UNE 83952. Concrete durability. Water for mixing and aggressive waters. Determination of the pH. Potentiometric method. Madrid, Spain 2008.
- AENOR. UNE-EN 196-1. Methods of testing cement - Part 1: Determination of strength. Madrid, Spain2018.
- Sáez Blázquez C, Farfán Martín A, Martín Nieto I, Carrasco García P, Sánchez Pérez LS, González-Aguilera D. Efficiency analysis of the main components of a vertical closed-loop system in a borehole heat exchanger. Energies. 2017;10:201 1996-073.
- Devices D. KD2 Pro thermal properties analyzer operator's manual. USA: WA; 2016.
- Tawfik M, Tonnellier X, Sansom C. Light source selection for a solar simulator for thermal applications: A review. Renew Sustain Energy Rev. 2018;90:802-13 1364-0321.
- Colarossi D, Tagliolini E, Principi P, Fioretti R. Design and validation of an adjustable large-scale solar simulator. Appl Sci 2021;11:1964.